Journal of Computational and Applied Mathematics 224 (2009) 646–657

Contents lists available at ScienceDirect

Journal of Computational and Applied Mathematics

journal homepage: www.elsevier.com/locate/cam

Damageable contact between an elastic body and a rigid foundation☆

M. Campo, J.R. Fernández *, A. Silva

Departamento de Matemática Aplicada, Universidade de Santiago de Compostela, Facultade de Matemáticas, Campus Sur s/n, 15782 Santiago de Compostela, Spain

ARTICLE INFO

Article history:
Received 11 June 2007
Received in revised form 22 May 2008

Keywords:
Quasistatic elastic problem
Damage
Signorini contact conditions
Error estimates
Numerical simulations

ABSTRACT

In this work, the contact problem between an elastic body and a rigid obstacle is studied, including the development of material damage which results from internal compression or tension. The variational problem is formulated as a first-kind variational inequality for the displacements coupled with a parabolic partial differential equation for the damage field. The existence of a unique local weak solution is stated. Then, a fully discrete scheme is introduced using the finite element method to approximate the spatial variable and an Euler scheme to discretize the time derivatives. Error estimates are derived on the approximate solutions, from which the linear convergence of the algorithm is deduced under suitable regularity conditions. Finally, three two-dimensional numerical simulations are performed to demonstrate the accuracy and the behaviour of the scheme.

1. Introduction

This work deals with the numerical analysis of a quasistatic contact problem between an elastic body and a rigid obstacle, the so-called foundation. The damage of the material, caused by the opening and growth of micro-cracks and micro-cavities, is also taken into account since it leads to the decrease in the load carrying capacity of the body and, eventually, to the possible failure of the system in which the body is situated.

Of course, when engineering structures are considered, such as tall buildings, bridges or dams, it is very important to predict the evolution of their mechanical damage because it affects the mechanical integrity, functioning, life-span, safety, and indirectly the warranty, of most engineering systems. There exists very large engineering literature dealing with the many approaches and facets of material damage (see, e.g., [3,27–31,33,34]).

The novel idea of modelling material damage by the introduction of the *damage field* originated in the works of Frémond [15–17] and was motivated by the evolution of damage in concrete structures. These ideas have been extended recently in [1,2,5–7,11,14,18,20,26]. Additional results and references can be found in the recent monograph [32]. In this approach the damage field ζ varies between one and zero at each point in the body. When $\zeta = 1$ the material is damage-free, when $\zeta = 0$ the material is completely damaged, and for $0 < \zeta < 1$ it is partially damaged. The evolution of the damage field is described here by a parabolic partial differential equation.

In this work, since the contact is assumed frictionless and with a rigid body, the classical Signorini contact conditions are employed to model the process (see [23]). Therefore, the variational formulation of this problem is written as a coupled system which consists of a first-kind variational inequality for the displacement field and a linear parabolic variational equation for the evolution of the damage field. The existence of a unique weak solution to the problem is obtained using similar arguments to those employed in [8,24] for elastic-viscoplastic materials and assuming contact with a deformable obstacle. In this paper, we continue the investigation reported in [9], where the contact was not considered, and we notice

☆ This work was partially supported by the Ministerio de Educación y Ciencia (Project MTM2006-13981).
* Corresponding author. Tel.: +34 981563100x23244; fax: +34 982285926.
E-mail address: jramon@usc.es (J.R. Fernández).

0377-0427/$ – see front matter © 2008 Elsevier B.V. All rights reserved.
doi:10.1016/j.cam.2008.05.046

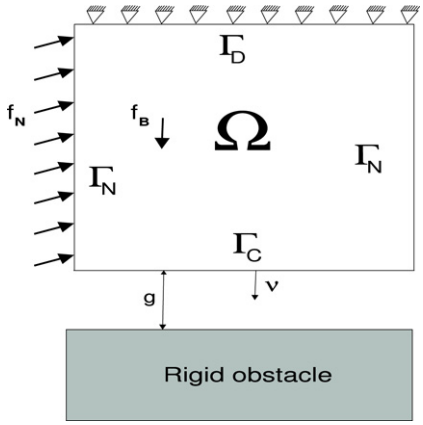

Fig. 1. A frictionless contact problem between an elastic body and a rigid obstacle.

that the novelty of this work is the numerical algorithm, its error estimates, and its implementations which lead to numerical simulations of the model.

The rest of the paper is structured as follows. The mechanical model and its weak formulation are presented in Section 2. The assumptions on the problem data and the statement of the existence and uniqueness of the weak solution, Theorem 2, are also given. In Section 3, a fully discrete scheme is introduced based on the finite element method to approximate the spatial variable and an Euler scheme to discretize the time derivatives. Error estimates are provided in Theorem 6, from which, under suitable regularity conditions, the linear convergence of the fully discrete approximation is deduced. Finally, two-dimensional numerical examples are described in Section 4 in order to demonstrate the performance of the algorithm and the behaviour of the solution.

2. Mechanical problem and variational formulation

Let $\mathbb{S}^d$, $d = 1, 2, 3$, be the space of symmetric $d \times d$ matrices with the usual notation of inner product.

We consider an elastic body which occupies a domain $\Omega \subset \mathbb{R}^d$ with outer surface $\partial\Omega = \Gamma = \Gamma_D \cup \Gamma_N \cup \Gamma_C$ which is assumed to be sufficiently smooth. Also the boundary parts Γ_D, Γ_N and Γ_C are disjoint subsets and Γ_D and Γ_C have positive surface measures. For each $\boldsymbol{x} \in \Gamma$, let $\boldsymbol{\nu}(\boldsymbol{x})$ denote the unit normal outward vector to Γ. Volume forces of density $\boldsymbol{f}_B$ act in $\Omega \times (0, T)$, for a final time $T > 0$, and tractions of density $\boldsymbol{f}_N$ act on Γ_N. Finally, the body may come into contact with a rigid obstacle over the boundary part Γ_C. A gap g exists between the potential contact surface Γ_C and the obstacle, and it is measured along $\boldsymbol{\nu}$ (see Fig. 1).

We denote by $\boldsymbol{u}$ the displacement field, $\boldsymbol{\sigma}$ the stress tensor, and $\boldsymbol{\varepsilon}(\boldsymbol{u})$ the linearized strain tensor given by

$$\boldsymbol{\varepsilon}(\boldsymbol{u}) = (\varepsilon_{ij}(\boldsymbol{u}))_{i,j=1}^{d}, \qquad \varepsilon_{ij}(\boldsymbol{u}) = \frac{1}{2}\left(\frac{\partial u_i}{\partial x_j} + \frac{\partial u_j}{\partial x_i}\right).$$

We let ζ denote the damage field, which is defined in $\Omega \times (0, T)$ and measures the fractional decrease in the strength of the material. The material is assumed elastic satisfying the following constitutive law (see, e.g., [13,32]),

$$\boldsymbol{\sigma} = \zeta\, \mathcal{A}\boldsymbol{\varepsilon}(\boldsymbol{u}),$$

where $\mathcal{A} = (a_{ijkl})_{i,j,k,l=1}^{d}$ is a prescribed fourth-order tensor, and we notice that the classical linear elasticity theory is obtained when $\zeta = 1$.

Let us present briefly the contact model. The classical frictionless Signorini conditions are written as follows (see [23]),

$$\boldsymbol{\sigma}_\tau = \boldsymbol{0}, \quad u_\nu - g \le 0, \quad \sigma_\nu \le 0, \quad \sigma_\nu(u_\nu - g) = 0 \quad \text{on } \Gamma_C \times (0, T),$$

where $u_\nu = \boldsymbol{u} \cdot \boldsymbol{\nu}$ denotes the normal displacements, and $\sigma_\nu = \boldsymbol{\sigma}\boldsymbol{\nu} \cdot \boldsymbol{\nu}$ and $\boldsymbol{\sigma}_\tau = \boldsymbol{\sigma}\boldsymbol{\nu} - \sigma_\nu \boldsymbol{\nu}$ are the normal and tangential stresses, respectively.

We now describe the damage process. As a result of the tensile or compressive stresses in the body, micro-cracks and micro-cavities open and grow and this causes the load bearing capacity of the material to decrease. This reduction in the strength of an isotropic material is modelled by introducing the damage field $\zeta = \zeta(\boldsymbol{x}, t)$ as the ratio

$$\zeta = \zeta(\boldsymbol{x}, t) = \frac{E_{eff}}{E},$$

between the effective modulus of elasticity E_{eff} and that of the damage-free material E. It follows from this definition that the damage field is constrained to the values $0 \le \zeta \le 1$.

Following the derivation presented in [15,16] (see [17] for full details), the evolution of the microscopic cracks and cavities responsible for the damage is described by the following parabolic partial differential equation,

$$\zeta' - \kappa \Delta \zeta = \phi(\boldsymbol{\varepsilon}(\boldsymbol{u}), \zeta) \quad \text{in } \Omega \times (0, T).$$

Here, the prime denotes the time derivative, $\triangle$ is the Laplace operator, $\kappa > 0$ is the damage diffusion constant and ϕ is the damage source function whose properties will be described below.

We assume that there is no damage influx throughout the boundary Γ and therefore, $\partial\zeta/\partial\boldsymbol{\nu} = 0$ there. It is straightforward to extend the results presented below to more general situations.

For technical reasons associated with the loss of coercivity in the elastic equation, and possible singularities in ϕ as $\zeta \to 0$, we introduce the truncation operator $\eta_* : \mathbb{R} \to \mathbb{R}$. This is a nondecreasing $C(\Omega)$-function which satisfies, for fixed $\zeta_* > 0$,

$$\eta_*(\zeta) = \begin{cases} 1 & \text{if } \zeta > 1, \\ \zeta & \text{if } \zeta_* \le \zeta \le 1, \\ \zeta_* & \text{if } \zeta < \zeta_*. \end{cases}$$

We note that as long as $\zeta \in [\zeta_*, 1]$ it makes no difference whether we use ζ or $\eta_*(\zeta)$. The purpose of using η_* is to allow us to obtain global regular solutions (see [25]).

Remark 1. We note that when the damage function is close to zero, i.e., the damage is substantial, the material is dense with micro-cracks (it is likely to develop a crack) and modelling it as an elastic material ceases to make sense. Therefore, we postulate the existence of such a lower limit for the damage, denoted by $\zeta_* > 0$. Moreover, this condition is also required for the numerical analysis of the problem since it guarantees that the stiffness matrix is positive definite.

Thus, the mechanical form of the quasistatic contact problem between an elastic body and a rigid obstacle, including the damage of the material, is the following.

Problem P. Find a displacement field $\boldsymbol{u} : \Omega \times (0, T) \to \mathbb{R}^d$, a stress field $\boldsymbol{\sigma} : \Omega \times (0, T) \to \mathbb{S}^d$, and a damage field $\zeta : \Omega \times (0, T) \to \mathbb{R}$ such that,

$$-\mathrm{Div}\,\boldsymbol{\sigma} = \boldsymbol{f}_B \quad \text{in } \Omega \times (0, T), \tag{1}$$

$$\boldsymbol{\sigma} = \eta_*(\zeta)\,\mathcal{A}\boldsymbol{\varepsilon}(\boldsymbol{u}) \quad \text{in } \Omega \times (0, T), \tag{2}$$

$$\zeta' - \kappa \Delta \zeta = \phi(\boldsymbol{\varepsilon}(\boldsymbol{u}), \eta_*(\zeta)) \quad \text{in } \Omega \times (0, T), \tag{3}$$

$$\frac{\partial \zeta}{\partial \boldsymbol{\nu}} = 0 \quad \text{on } \Gamma \times (0, T), \tag{4}$$

$$\boldsymbol{u} = \boldsymbol{0} \quad \text{on } \Gamma_D \times (0, T), \tag{5}$$

$$\boldsymbol{\sigma}\boldsymbol{\nu} = \boldsymbol{f}_N \quad \text{on } \Gamma_N \times (0, T), \tag{6}$$

$$\boldsymbol{\sigma}_\tau = \boldsymbol{0} \quad \text{on } \Gamma_C \times (0, T), \tag{7}$$

$$u_\nu - g \le 0, \quad \sigma_\nu \le 0, \quad \sigma_\nu(u_\nu - g) = 0 \quad \text{on } \Gamma_C \times (0, T), \tag{8}$$

$$\zeta(0) = \zeta_0 \quad \text{in } \Omega. \tag{9}$$

We now present the variational formulation of the problem. To that end we introduce the following spaces and notation. Let $Y = L^2(\Omega)$, $E = H^1(\Omega)$, $H = [L^2(\Omega)]^d$, and denote by Q the space of second order symmetric tensor functions,

$$Q = \left\{ \boldsymbol{\tau} \in [L^2(\Omega)]^{d\times d};\ \tau_{ij} = \tau_{ji} \right\}.$$

Let V be defined by

$$V = \{\boldsymbol{v} \in [H^1(\Omega)]^d;\ \boldsymbol{v} = \boldsymbol{0} \text{ on } \Gamma_D\},$$

and define the admissible displacement convex set U as,

$$U = \{\boldsymbol{v} \in V;\ v_\nu = \boldsymbol{v}\cdot\boldsymbol{\nu} \le g \text{ on } \Gamma_C\}.$$

We now describe the assumptions on the problem data.

The fourth-order elasticity tensor $\mathcal{A} = (a_{ijkl})_{i,j,k,l=1}^d : \Omega \times \mathbb{S}^d \to \mathbb{S}^d$ satisfies:

$$a_{ijkl}(\boldsymbol{x}) = a_{klij}(\boldsymbol{x}) = a_{jikl}(\boldsymbol{x}) \quad \text{for } i, j, k, l = 1, \ldots, d. \tag{10}$$

$$\mathcal{A}(\boldsymbol{x})\,\boldsymbol{\tau}\cdot\boldsymbol{\tau} \ge m_{\mathcal{A}}\,|\boldsymbol{\tau}|^2_{\mathbb{S}^d}, \quad \text{for all } \boldsymbol{\tau} \in \mathbb{S}^d. \tag{11}$$

$$\text{The mapping } \boldsymbol{x} \to \mathcal{A}(\boldsymbol{x}) \text{ is measurable and bounded.} \tag{12}$$

The damage source function $\phi : \Omega \times \mathbb{S}^d \times \mathbb{R} \to \mathbb{R}$ is Lipschitz and verifies:

$$|\phi(\boldsymbol{x}, \boldsymbol{\varepsilon}_1, \eta_*(\zeta_1)) - \phi(\boldsymbol{x}, \boldsymbol{\varepsilon}_2, \eta_*(\zeta_2))| \le L_\phi(|\boldsymbol{\varepsilon}_1 - \boldsymbol{\varepsilon}_2| + |\eta_*(\zeta_1) - \eta_*(\zeta_2)|)$$

$$\text{for all } \boldsymbol{\varepsilon}_1, \boldsymbol{\varepsilon}_2 \in \mathbb{S}^d, \quad \zeta_1, \zeta_2 \in \mathbb{R}, \quad \text{a.e. } \boldsymbol{x} \in \Omega. \tag{13}$$

$$\text{The function } \boldsymbol{x} \to \phi(\boldsymbol{x}, \boldsymbol{\varepsilon}, \zeta) \text{ is measurable.} \tag{14}$$

$$\text{The mapping } \boldsymbol{x} \to \phi(\boldsymbol{x}, \boldsymbol{0}, 0) \text{ belongs to } Y. \tag{15}$$

$$\phi(\boldsymbol{x}, \boldsymbol{\varepsilon}, \eta_*(\zeta)) \text{ is bounded.} \tag{16}$$

$$\phi(\boldsymbol{x}, \boldsymbol{\varepsilon}, \zeta) \le 0 \quad \text{if } \zeta \ge 1, \quad \phi(\boldsymbol{x}, \boldsymbol{\varepsilon}, \zeta) \ge 0 \quad \text{if } \zeta \le \zeta_*. \tag{17}$$

Below, and in the rest of this work, we do not show the dependence of these functions on $\boldsymbol{x}$ in order to simplify the writing.

The density of body forces and the tractions are assumed to satisfy

$$\boldsymbol{f}_B \in C([0,T]; H), \quad \boldsymbol{f}_N \in C\left([0,T]; [L^2(\Gamma_N)]^d\right), \tag{18}$$

and we define the element $\boldsymbol{f} \in C([0,T]; V)$ by

$$(\boldsymbol{f}(t), \boldsymbol{w})_V = (\boldsymbol{f}_B(t), \boldsymbol{w})_H + (\boldsymbol{f}_N(t), \boldsymbol{w})_{[L^2(\Gamma_N)]^d} \quad \forall \boldsymbol{w} \in V.$$

In addition, we assume that the gap function and the initial condition satisfy,

$$\begin{aligned} &g \in L^2(\Gamma_C), \quad g(\boldsymbol{x}) \ge 0 \quad \text{for a.e. } \boldsymbol{x} \in \Gamma_C, \\ &\zeta_0 \in E, \quad \zeta_0(\boldsymbol{x}) \in (\zeta_*, 1] \quad \text{for a.e. } \boldsymbol{x} \in \Omega. \end{aligned} \tag{19}$$

To describe the variational form of the problem we need the bilinear form $a : E \times E \to \mathbb{R}$ given by

$$a(\xi, \eta) = \kappa \int_\Omega \nabla\xi \cdot \nabla\eta \, d\boldsymbol{x} \quad \forall \xi, \eta \in E.$$

Therefore, using a Green's formula, the variational formulation of the mechanical problem P is the following.

Problem *VP*. Find a displacement field $\boldsymbol{u} : [0,T] \to U$ and a damage field $\zeta : [0,T] \to E$ such that $\zeta(0) = \zeta_0$ and for a.e. $t \in [0,T]$,

$$(\eta_*(\zeta(t))\mathcal{A}\boldsymbol{\varepsilon}(\boldsymbol{u}(t)), \boldsymbol{\varepsilon}(\boldsymbol{v} - \boldsymbol{u}(t)))_Q \ge (\boldsymbol{f}(t), \boldsymbol{v} - \boldsymbol{u}(t))_V \quad \forall \boldsymbol{v} \in U, \tag{20}$$

$$(\zeta'(t), \xi)_Y + a(\zeta(t), \xi) = (\phi(\boldsymbol{\varepsilon}(\boldsymbol{u}(t)), \zeta(t)), \xi)_Y \quad \forall \xi \in E. \tag{21}$$

The following theorem, which states the existence of a unique solution to Problem *VP*, is obtained by using similar arguments to those employed in [24,25].

Theorem 2. *Assume that (10)–(19) hold. Then, there exists a unique solution to Problem VP such that*

$$\begin{aligned} &\zeta \in L^2(0,T; H^2(\Omega)) \cap H^1(0,T; Y), \\ &\zeta(\boldsymbol{x}, t) \in [\zeta_*, 1] \quad \textit{for a.e. } (\boldsymbol{x}, t) \in \Omega \times (0,T), \\ &\boldsymbol{u} \in L^\infty(0,T; U). \end{aligned}$$

The proof of the theorem was based on the regularization of the variational problem and a priori estimates.

3. Fully discrete approximations: Error estimates

In this section we introduce a finite element algorithm for the solution to Problem *VP* and we obtain an error estimate on the approximate solutions.

The discretization of Problem *VP* will be done in two steps. First, we consider two finite-dimensional spaces $V^h \subset V$ and $E^h \subset E$ which approximate the spaces V and E, respectively. Here, $h > 0$ denotes the spatial discretization parameter. The discrete admissible displacement convex set is then defined as $U^h = U \cap V^h$.

Remark 3. In the numerical simulations described in the following section, V^h and E^h consist of continuous and piecewise affine functions; that is,

$$V^h = \{\boldsymbol{v}^h \in [C(\overline{\Omega})]^d; \boldsymbol{v}^h_{|_{Tr}} \in [P_1(Tr)]^d \ \forall Tr \in \mathcal{T}^h, \boldsymbol{v}^h = \boldsymbol{0} \quad \text{on } \Gamma_D\}, \tag{22}$$

$$E^h = \{\xi^h \in C(\overline{\Omega}); \xi^h_{|_{Tr}} \in P_1(Tr) \ \forall Tr \in \mathcal{T}^h\}, \tag{23}$$

where Ω is assumed to be a polygonal domain, $\mathcal{T}^h$ denotes a finite element triangulation of $\overline{\Omega}$ and $P_1(Tr)$ represents the space of polynomial functions of global degree less than or equal to 1 in Tr. Therefore, we notice that the discrete convex set U^h is defined as,

$$U^h = \{\boldsymbol{v}^h \in V^h; v^h_\nu = \boldsymbol{v}^h \cdot \boldsymbol{\nu} \le g \text{ on } \Gamma_C\}. \tag{24}$$

To discretize the time derivatives, we consider a uniform partition of the time interval $[0, T]$, denoted by $0 = t_0 < t_1 < \cdots < t_N = T$ and let k be the time step size, $k = T/N$. For a continuous function $f(t)$, let $f_n = f(t_n)$ and for a sequence $\{w_n\}_{n=0}^N$ we let $\delta w_n = (w_n - w_{n-1})/k$ be its corresponding divided differences.

The fully discrete approximation of Problem *VP*, based on a hybrid combination of the backward and the forward Euler schemes, is as follows.

Problem VP^{hk}. Find a discrete displacement field $\boldsymbol{u}^{hk} = \{\boldsymbol{u}_n^{hk}\}_{n=0}^N \subset U^h$ and a discrete damage field $\zeta^{hk} = \{\zeta_n^{hk}\}_{n=0}^N \subset E^h$ such that $\zeta_0^{hk} = \zeta_0^h$ and for all $\xi^h \in E^h$, $\boldsymbol{v}^h \in U^h$ and $n = 1, 2, \ldots, N$,

$$(\delta\zeta_n^{hk}, \xi^h)_Y + a(\zeta_n^{hk}, \xi^h) = (\phi(\boldsymbol{\varepsilon}(\boldsymbol{u}_{n-1}^{hk}), \zeta_{n-1}^{hk}), \xi^h)_Y, \tag{25}$$

$$(\eta_*(\zeta_n^{hk})\mathcal{A}\boldsymbol{\varepsilon}(\boldsymbol{u}_n^{hk}), \boldsymbol{\varepsilon}(\boldsymbol{v}^h - \boldsymbol{u}_n^{hk}))_Q \geq (\boldsymbol{f}_n, \boldsymbol{v}^h - \boldsymbol{u}_n^{hk})_V, \tag{26}$$

where ζ_0^h is an appropriate approximation of the initial condition ζ_0, and $\boldsymbol{u}_0^{hk} \in U^h$ is the unique solution to the following problem,

$$(\eta_*(\zeta_0^h)\mathcal{A}\boldsymbol{\varepsilon}(\boldsymbol{u}_0^{hk}), \boldsymbol{\varepsilon}(\boldsymbol{v}^h - \boldsymbol{u}_0^{hk}))_Q \geq (\boldsymbol{f}_0, \boldsymbol{v}^h - \boldsymbol{u}_0^{hk})_V \quad \forall \boldsymbol{v}^h \in U^h. \tag{27}$$

Using standard arguments for variational inequalities (see [19]), we deduce the existence and uniqueness of the solution to Problem VP^{hk}, which we state as follows.

Theorem 4. *Let the assumptions of Theorem 2 hold. Then, there exists a unique solution to Problem* VP^{hk} *such that* $\boldsymbol{u}^{hk} \subset U^h$ *and* $\zeta^{hk} \subset E^h$.

Remark 5. We notice that the above discrete problem is a decoupled system composed of a linear variational equation for the discrete damage field and a first-kind variational inequality for the discrete displacements. First, the discrete initial displacements are obtained solving the discrete variational inequality (27). A penalty-duality algorithm, introduced in [4] and already applied in other contact problems, is used for its numerical resolution.

Then, we rewrite (25) in the form

$$\zeta_n^{hk} \in E^h, \quad (\zeta_n^{hk}, \xi^h)_Y + ka(\zeta_n^{hk}, \xi^h) = k(\phi(\boldsymbol{\varepsilon}(\boldsymbol{u}_{n-1}^{hk}), \zeta_{n-1}^{hk}), \xi^h)_Y + (\zeta_{n-1}^{hk}, \xi^h)_Y \quad \forall \xi^h \in E^h. \tag{28}$$

Eq. (28) is a linear system that is solved using Cholesky's method.

Once ζ_n^{hk} is calculated, it is introduced into (26). In practice, $\zeta_n^{hk} > \zeta_*$ (since the program stops when the value ζ_* is reached) and therefore, Eq. (26) leads to a first-kind variational inequality which is again solved by using the above penalty-duality algorithm.

Our interest here lies in estimating the numerical errors $\|\boldsymbol{u}_n - \boldsymbol{u}_n^{hk}\|_V$ and $\|\zeta_n - \zeta_n^{hk}\|_Y$. Thus, let us assume the following regularity conditions on the continuous solution,

$$\begin{aligned} &\boldsymbol{u} \in C([0, T]; V), \\ &\boldsymbol{\varepsilon}(\boldsymbol{u}) \in L^\infty(0, T; [L^\infty(\Omega)]^{d\times d}), \\ &\zeta \in C([0, T]; E) \cap C^1([0, T]; Y). \end{aligned} \tag{29}$$

First, we take variational inequality (20) at time $t = t_n$ for $\boldsymbol{v} = \boldsymbol{u}_n^{hk} \in U^h \subset U$ to obtain,

$$(\eta_*(\zeta_n)\mathcal{A}\boldsymbol{\varepsilon}(\boldsymbol{u}_n), \boldsymbol{\varepsilon}(\boldsymbol{u}_n^{hk} - \boldsymbol{u}_n))_Q \geq (\boldsymbol{f}_n, \boldsymbol{u}_n^{hk} - \boldsymbol{u}_n)_V.$$

Then, we rewrite the discrete variational inequality (26) in the following form,

$$(\eta_*(\zeta_n^{hk})\mathcal{A}\boldsymbol{\varepsilon}(\boldsymbol{u}_n^{hk}), \boldsymbol{\varepsilon}(\boldsymbol{u}_n - \boldsymbol{u}_n^{hk}))_Q \geq (\boldsymbol{f}_n, \boldsymbol{v}^h - \boldsymbol{u}_n^{hk})_V + (\eta_*(\zeta_n^{hk})\mathcal{A}\boldsymbol{\varepsilon}(\boldsymbol{u}_n^{hk}), \boldsymbol{\varepsilon}(\boldsymbol{u}_n - \boldsymbol{v}^h))_Q \quad \forall \boldsymbol{v}^h \in U^h,$$

and adding the above two inequalities we find that

$$(\eta_*(\zeta_n)\mathcal{A}\boldsymbol{\varepsilon}(\boldsymbol{u}_n) - \eta_*(\zeta_n^{hk})\mathcal{A}\boldsymbol{\varepsilon}(\boldsymbol{u}_n^{hk}), \boldsymbol{\varepsilon}(\boldsymbol{u}_n - \boldsymbol{u}_n^{hk}))_Q \leq (\boldsymbol{f}_n, \boldsymbol{u}_n - \boldsymbol{v}^h)_V + (\eta_*(\zeta_n^{hk})\mathcal{A}\boldsymbol{\varepsilon}(\boldsymbol{u}_n^{hk}), \boldsymbol{\varepsilon}(\boldsymbol{v}^h - \boldsymbol{u}_n))_Q \quad \forall \boldsymbol{v}^h \in U^h.$$

Let us bound the left-hand side of the above inequality. Writing it as follows,

$$\begin{aligned}(\eta_*(\zeta_n)\mathcal{A}\boldsymbol{\varepsilon}(\boldsymbol{u}_n) - \eta_*(\zeta_n^{hk})\mathcal{A}\boldsymbol{\varepsilon}(\boldsymbol{u}_n^{hk}), \boldsymbol{\varepsilon}(\boldsymbol{u}_n - \boldsymbol{u}_n^{hk}))_Q &= (\eta_*(\zeta_n^{hk})\mathcal{A}\boldsymbol{\varepsilon}(\boldsymbol{u}_n - \boldsymbol{u}_n^{hk}), \boldsymbol{\varepsilon}(\boldsymbol{u}_n - \boldsymbol{u}_n^{hk}))_Q \\ &+ ((\eta_*(\zeta_n) - \eta_*(\zeta_n^{hk}))\mathcal{A}\boldsymbol{\varepsilon}(\boldsymbol{u}_n), \boldsymbol{\varepsilon}(\boldsymbol{u}_n - \boldsymbol{u}_n^{hk}))_Q,\end{aligned}$$

keeping in mind that

$$(\eta_*(\zeta_n^{hk})\mathcal{A}\boldsymbol{\varepsilon}(\boldsymbol{u}_n^{hk}), \boldsymbol{\varepsilon}(\boldsymbol{v}^h - \boldsymbol{u}_n))_Q = (\eta_*(\zeta_n^{hk})\mathcal{A}\boldsymbol{\varepsilon}(\boldsymbol{u}_n), \boldsymbol{\varepsilon}(\boldsymbol{v}^h - \boldsymbol{u}_n))_Q + (\eta_*(\zeta_n^{hk})\mathcal{A}\boldsymbol{\varepsilon}(\boldsymbol{u}_n^{hk} - \boldsymbol{u}_n), \boldsymbol{\varepsilon}(\boldsymbol{v}^h - \boldsymbol{u}_n))_Q,$$

applying several times the inequality

$$ab \leq \epsilon a^2 + \frac{1}{4\epsilon}b^2, \quad a, b, \epsilon \in \mathbb{R}, \epsilon > 0, \tag{30}$$

and using the regularity $\boldsymbol{\varepsilon}(\boldsymbol{u}) \in L^\infty(0,T;[L^\infty(\Omega)]^{d\times d})$ and the properties $\eta_*(\zeta_n)$, $\eta_*(\zeta_n^{hk}) > \eta_*$, $\eta_*(\zeta_n)$, $\eta_*(\zeta_n^{hk}) \le 1$, we find that

$$\|\boldsymbol{u}_n - \boldsymbol{u}_n^{hk}\|_V^2 \le c(\|\zeta_n - \zeta_n^{hk}\|_Y^2 + \|\boldsymbol{u}_n - \boldsymbol{v}^h\|_V + \|\boldsymbol{u}_n - \boldsymbol{v}^h\|_V^2) \quad \forall \boldsymbol{v}^h \in U^h. \tag{31}$$

Here and below, c is a constant which depends on the problem data and the continuous solution, but it is independent of k or h.

We turn now to obtain an error estimate for the damage field. It was already done in [9] and we refer the reader there for further details. We sketch below the proof.

Let us denote by $\phi_n = \phi(\boldsymbol{\varepsilon}(\boldsymbol{u}_n), \zeta_n)$ and $\phi_{n-1}^{hk} = \phi(\boldsymbol{\varepsilon}(\boldsymbol{u}_{n-1}^{hk}), \zeta_{n-1}^{hk})$. Writing Eq. (21) at time $t = t_n$ for all $\xi = \xi^h \in E^h$ and subtracting it from Eq. (25), it follows that

$$\begin{aligned}
&(\zeta_n' - \delta\zeta_n^{hk}, \zeta_n - \zeta_n^{hk})_Y + a(\zeta_n - \zeta_n^{hk}, \zeta_n - \zeta_n^{hk}) - (\phi_n - \phi_{n-1}^{hk}, \zeta_n - \zeta_n^{hk})_Y \\
&\quad = (\zeta_n' - \delta\zeta_n^{hk}, \zeta_n - \xi^h)_Y + a(\zeta_n - \zeta_n^{hk}, \zeta_n - \xi^h) - (\phi_n - \phi_{n-1}^{hk}, \zeta_n - \xi^h)_Y,
\end{aligned}$$

for all $\xi^h \in E^h$. Then, after some manipulations, we get

$$\begin{aligned}
&(\delta\zeta_n - \delta\zeta_n^{hk}, \zeta_n - \zeta_n^{hk})_Y + c\|\nabla(\zeta_n - \zeta_n^{hk})\|_H^2 \le c(\|\boldsymbol{u}_n - \boldsymbol{u}_{n-1}^{hk}\|_V + \|\zeta_n - \zeta_{n-1}^{hk}\|_Y)\|\zeta_n - \zeta_n^{hk}\|_Y \\
&\quad + \|\zeta_n' - \delta\zeta_n\|_Y(\|\zeta_n - \zeta_n^{hk}\|_Y + \|\zeta_n - \xi^h\|_Y) + \|\nabla(\zeta_n - \zeta_n^{hk})\|_H\|\zeta_n - \xi^h\|_E \\
&\quad + c(\|\boldsymbol{u}_n - \boldsymbol{u}_{n-1}^{hk}\|_V + \|\zeta_n - \zeta_{n-1}^{hk}\|_Y)\|\zeta_n - \xi^h\|_Y + (\delta\zeta_n - \delta\zeta_n^{hk}, \zeta_n - \xi^h)_Y,
\end{aligned}$$

where $\delta\zeta_n = (\zeta_n - \zeta_{n-1})/k$. Since

$$(\delta\zeta_n - \delta\zeta_n^{hk}, \zeta_n - \zeta_n^{hk})_Y \ge \frac{1}{2k}\left[\|\zeta_n - \zeta_n^{hk}\|_Y^2 - \|\zeta_{n-1} - \zeta_{n-1}^{hk}\|_Y^2\right],$$

using inequality (30) several times, by induction it leads to the following estimate,

$$\begin{aligned}
\|\zeta_n - \zeta_n^{hk}\|_Y^2 + k\sum_{j=1}^n \|\nabla(\zeta_j - \zeta_j^{hk})\|_H^2 &\le ck\sum_{j=1}^n \big(\|\boldsymbol{u}_{j-1} - \boldsymbol{u}_{j-1}^{hk}\|_V^2 + \|\zeta_{j-1} - \zeta_{j-1}^{hk}\|_Y^2 \\
&\quad + \|\zeta_j' - \delta\zeta_j\|_Y^2 + \|\boldsymbol{u}_j - \boldsymbol{u}_{j-1}\|_V^2 + \|\zeta_j - \zeta_{j-1}\|_Y^2 + \|\zeta_j - \xi_j^h\|_E^2\big) \\
&\quad + c\sum_{j=1}^n (\zeta_j - \zeta_j^{hk} - (\zeta_{j-1} - \zeta_{j-1}^{hk}), \zeta_j - \xi_j^h)_Y + \|\zeta_0 - \zeta_0^h\|_Y^2,
\end{aligned}$$

for all $\xi^h = \{\xi_j^h\}_{j=0}^n \subset E^h$. Taking into account that

$$\begin{aligned}
\sum_{j=1}^n (\zeta_j - \zeta_j^{hk} - (\zeta_{j-1} - \zeta_{j-1}^{hk}), \zeta_j - \xi_j^h)_Y &\le \epsilon\|\zeta_n - \zeta_n^{hk}\|_Y^2 + c\|\zeta_n - \xi_n^h\|_Y^2 + c\|\zeta_0 - \zeta_0^h\|_Y^2 + c\|\zeta_1 - \xi_1^h\|_Y^2 \\
&\quad + k\sum_{j=1}^{n-1}\|\zeta_j - \zeta_j^{hk}\|_Y^2 + \frac{1}{k}\sum_{j=1}^{n-1}\|\zeta_j - \xi_j^h - (\zeta_{j+1} - \xi_{j+1}^h)\|_Y^2,
\end{aligned}$$

where $\epsilon > 0$ is assumed sufficiently small, we have the following error estimate, for all $\xi^h = \{\xi_j^h\}_{j=1}^N \subset E^h$,

$$\begin{aligned}
&\|\zeta_n - \zeta_n^{hk}\|_Y^2 + k\sum_{j=1}^n \|\nabla(\zeta_j - \zeta_j^{hk})\|_H^2 \\
&\le c\left(k\sum_{j=1}^n \big\{\|\boldsymbol{u}_{j-1} - \boldsymbol{u}_{j-1}^{hk}\|_V^2 + \|\zeta_{j-1} - \zeta_{j-1}^{hk}\|_Y^2 + \|\zeta_j' - \delta\zeta_j\|_Y^2 + \|\boldsymbol{u}_j - \boldsymbol{u}_{j-1}\|_V^2 + \|\zeta_j - \zeta_{j-1}\|_Y^2 \right.\right. \\
&\qquad \left.\left. + \|\zeta_j - \xi_j^h\|_E^2\big\} + \|\zeta_n - \xi_n^h\|_Y^2 + \|\zeta_0 - \zeta_0^h\|_Y^2 + \|\zeta_1 - \xi_1^h\|_Y^2 + \frac{1}{k}\sum_{j=1}^{n-1}\|\zeta_j - \xi_j^h - (\zeta_{j+1} - \xi_{j+1}^h)\|_Y^2\right).
\end{aligned} \tag{32}$$

Combining (31) and (32) and using a discrete version of Gronwall's inequality (see [21]), it leads to the following.

Theorem 6. *Let the assumptions of Theorem 2 and the regularity conditions (29) hold. There exists a constant $c > 0$, independent of h and k, such that for all $\{\zeta_j^h\}_{j=1}^N \subset E^h$ and $\{\boldsymbol{v}_j^h\}_{j=1}^N \subset U^h$,*

$$\max_{0\le n\le N}\{\|\boldsymbol{u}_n - \boldsymbol{u}_n^{hk}\|_V^2 + \|\zeta_n - \zeta_n^{hk}\|_Y^2\} + k\sum_{j=1}^N \|\nabla(\zeta_j - \zeta_j^{hk})\|_H^2$$

$$\leq c\left(k\sum_{j=1}^{N}\left\{\|\zeta_j'-\delta\zeta_j\|_Y^2+\|\boldsymbol{u}_j-\boldsymbol{u}_{j-1}\|_V^2+\|\zeta_j-\zeta_{j-1}\|_Y^2+\|\zeta_j-\xi_j^h\|_E^2\right\}\right.$$
$$+\max_{0\leq n\leq N}\left[\|\zeta_n-\xi_n^h\|_Y^2+\|\boldsymbol{u}_n-\boldsymbol{v}_n^h\|_V+\|\boldsymbol{u}_n-\boldsymbol{v}_n^h\|_V^2\right]+\|\zeta_0-\zeta_0^h\|_Y^2$$
$$\left.+\|\boldsymbol{u}_0-\boldsymbol{u}_0^{hk}\|_V^2+\frac{1}{k}\sum_{j=1}^{N-1}\|\zeta_j-\xi_j^h-(\zeta_{j+1}-\xi_{j+1}^h)\|_Y^2\right).$$

These error estimates are the basis for the analysis of the convergence rate of the algorithm.

As an example, let Ω be a polyhedral domain and denote by $\mathcal{T}^h$ a regular triangulation of $\overline{\Omega}$ compatible with the partition of the boundary $\Gamma=\partial\Omega$ into Γ_D, Γ_N and Γ_C. Let the finite element spaces V^h and E^h and the discrete convex set U^h be defined by (22), (23) and (24), respectively, and assume that the discrete initial condition ζ_0^h is obtained by $\zeta_0^h=\pi^h\zeta_0$, where $\pi^h: C(\overline{\Omega})\to E^h$ is the standard finite element interpolation operator (see, e.g., [12]). Moreover, we recall that the discrete initial displacements $\boldsymbol{u}_0^{hk}$ are the unique solution to the discrete variational inequality (27).

The following error estimates establish some convergence orders of the algorithm, with respect to the discretization parameters h and k, under suitable regularity conditions.

Corollary 7. *Let the assumptions of Theorem 6 hold. Under the following regularity conditions*

$$\boldsymbol{u}\in C([0,T];[H^2(\Omega)]^d)\cap C^1([0,T];V),$$
$$\zeta\in C([0,T];H^2(\Omega))\cap H^2(0,T;Y)\cap H^1(0,T;E),$$

there exists $c>0$, independent of h and k, such that,

$$\max_{0\leq n\leq N}\{\|\boldsymbol{u}_n-\boldsymbol{u}_n^{hk}\|_V+\|\zeta_n-\zeta_n^{hk}\|_Y\}\leq c(h^{1/2}+k). \tag{33}$$

Moreover, if we also assume that

$$\sigma_\nu\in C([0,T];L^2(\Gamma_C)),\quad u_\nu\in C([0,T];H^2(\Gamma_C)), \tag{34}$$

the numerical algorithm introduced in Problem VP^{hk} is linearly convergent; that is, there exists $c>0$, independent of h and k, such that,

$$\max_{0\leq n\leq N}\{\|\boldsymbol{u}_n-\boldsymbol{u}_n^{hk}\|_V+\|\zeta_n-\zeta_n^{hk}\|_Y\}\leq c(h+k). \tag{35}$$

Proof. First, we need to estimate the errors provided by the approximation of the finite element spaces V^h and E^h. Since $\boldsymbol{u}\in C([0,T];[H^2(\Omega)]^d)$ and $\zeta\in C([0,T];H^2(\Omega))$, we have (see [12]),

$$\max_{1\leq n\leq N}\inf_{v_n^h\in V^h}\|\boldsymbol{u}_n-\boldsymbol{v}_n^h\|_V\leq ch\|\boldsymbol{u}\|_{C([0,T];[H^2(\Omega)]^d)},$$
$$\max_{0\leq n\leq N}\inf_{\xi_n^h\in E^h}\|\zeta_n-\xi_n^h\|_E\leq ch\|\zeta\|_{C([0,T];H^2(\Omega))},$$

and, from (31) and the definition of the operator π^h we immediately obtain (see again [12]),

$$\|\boldsymbol{u}_0-\boldsymbol{u}_0^{hk}\|_V^2\leq c(h^2\|\zeta_0\|_{H^2(\Omega)}^2+h^2\|\boldsymbol{u}_0\|_{[H^2(\Omega)]^d}^2+h\|\boldsymbol{u}_0\|_{[H^2(\Omega)]^d}),$$
$$\|\zeta_0-\zeta_0^h\|_Y\leq ch^2\|\zeta_0\|_{H^2(\Omega)}.$$

Since $\boldsymbol{u}\in C^1([0,T];V)$ and $\zeta\in H^2(0,T;Y)$, it is easy to check that

$$\zeta_j'-\delta\zeta_j=\frac{1}{k}\int_{t_{j-1}}^{t_j}\int_{t_j}^{t}\zeta(s)\mathrm{d}s\mathrm{d}t,$$
$$\boldsymbol{u}_j-\boldsymbol{u}_{j-1}=k\boldsymbol{u}'(t)\quad t\in[t_{j-1},t_j],$$
$$\zeta_j-\zeta_{j-1}=k\zeta'(t)\quad t\in[t_{j-1},t_j],$$

and therefore,

$$k\sum_{j=1}^{N}\left[\|\zeta_j'-\delta\zeta_j\|_Y^2+\|\boldsymbol{u}_j-\boldsymbol{u}_{j-1}\|_V^2+\|\zeta_j-\zeta_{j-1}\|_Y^2\right]\leq ck^2(\|\boldsymbol{u}\|_{C^1([0,T];V)}^2+\|\zeta\|_{H^2(0,T;Y)}^2).$$

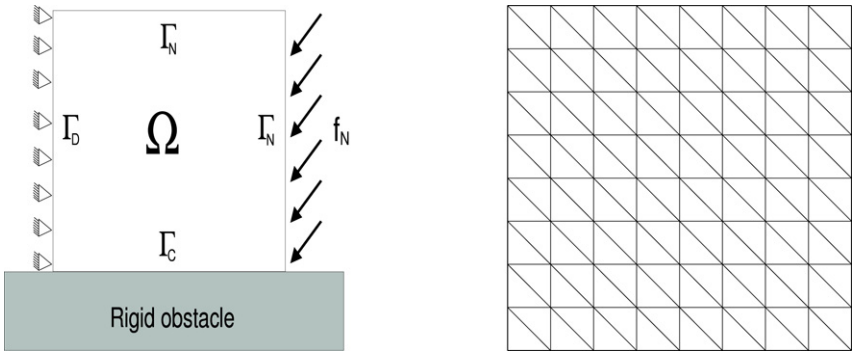

Fig. 2. Example I: Physical setting and mesh for $n = 8$.

Finally, in [20] the following estimate was obtained,

$$\frac{1}{k}\sum_{j=1}^{N-1} \|\zeta_j - \zeta_j^{hk} - (\zeta_{j+1} - \zeta_{j+1}^{hk})\|_Y^2 \leq ch^2 \|\zeta\|_{H^1(0,T;E)}^2,$$

which concludes the proof of (33).

The linear convergence (35) is now obtained proceeding as in [21], integrating by parts the equilibrium equation (1), using regularity conditions (34) and the following error estimate (see again [12]),

$$\max_{1\leq n\leq N} \inf_{v_n^h \in V^h} \|(\boldsymbol{u}_n - \boldsymbol{v}_n^h)\cdot \boldsymbol{v}\|_{L^2(\Gamma_C)} \leq ch^2 \|u_v\|_{C([0,T];H^2(\Gamma_C))}. \quad \square$$

4. Numerical results

To exhibit the performance of the numerical scheme we present some numerical results of its implementation.

In all the examples $\mathcal{A}\boldsymbol{\varepsilon}(\boldsymbol{u})$ was chosen as the two-dimensional plane-stress elasticity tensor,

$$(\mathcal{A}\boldsymbol{\tau})_{\alpha\beta} = \frac{Er}{1-r^2}(\tau_{11}+\tau_{22})\delta_{\alpha\beta} + \frac{E}{1+r}\tau_{\alpha\beta},$$

where $\alpha, \beta = 1, 2$, E and r are Young's modulus and Poisson's ratio, respectively, and $\delta_{\alpha\beta}$ denotes the Kronecker symbol.

The finite element spaces V^h and E^h and the discrete convex set U^h given by (22), (23) and (24), respectively, were employed and we also considered the damage source function ϕ defined as,

$$\phi(\boldsymbol{\varepsilon}(\boldsymbol{u}), \zeta) = -\left(\lambda_D\left(\frac{1-\zeta}{\zeta}\right) + \frac{1}{2}\lambda_U \Psi_{q^*}(\boldsymbol{\varepsilon}(\boldsymbol{u})) - \lambda_W\right)_+,$$

where λ_D, λ_U and λ_W are process parameters and the truncation function $\Psi : \mathbb{S}^d \to \mathbb{R}$ is given by

$$\Psi_{q^*}(\boldsymbol{\tau}) = \begin{cases} |\boldsymbol{\tau}|_{\mathbb{S}^d}^2 & \text{if } |\boldsymbol{\tau}|_{\mathbb{S}^d}^2 \leq q^*, \\ q^* & \text{otherwise,} \end{cases}$$

and $|\boldsymbol{\tau}|_{\mathbb{S}^d}^2 = \sum_{i,j=1}^d \tau_{ij}^2$ for all $\boldsymbol{\tau} = (\tau_{ij})_{i,j=1}^d \in \mathbb{S}^d$. Value $q^* = 1000$ was employed in the simulations.

4.1. Example I: Numerical convergence

In order to verify the asymptotic behaviour of the numerical method presented in the previous section, a sequence of numerical solutions was computed following the physical setting described in Fig. 2. Uniform partitions were considered of both the time interval and the spatial domain (each side of the square $[0, 1] \times [0, 1]$ was divided into n equal parts), and the corresponding solutions were compared with the "exact solution" obtained with $k = 0.0001$ and $n = 256$. The boundary $\Gamma_D = \{0\} \times [0, 1]$ was supposed to be fixed, $\Gamma_C = [0, 1] \times \{0\}$ was in frictionless contact with a rigid foundation and Γ_N was divided into two parts: $\{1\} \times [0, 1]$, on which a density of surface tractions $\boldsymbol{f}_N$ acted, and $[0, 1] \times \{1\}$, which was traction-free. No volume forces were supposed to act on the body.

The following data were used in this example:

$$T = 1\,\text{s}, \quad g = 0\,\text{m}, \quad \boldsymbol{f}_B = \boldsymbol{0}\,\text{N/m}^3, \quad \boldsymbol{f}_N = (-10, -10)\,\text{N/m}^2,$$
$$E = 80\,\text{N/m}^2, \quad r = 0.3, \quad \lambda_D = 0.1, \quad \lambda_U = 100, \quad \lambda_W = 0,$$
$$\zeta_* = 0.01, \quad \kappa = 0.01, \quad \zeta_0 = 1.$$

Table 1
Example I: Numerical errors obtained with different n and k

	k				
n	0.02	0.01	0.005	0.002	0.001
4	0.03027	0.02931	0.02884	0.02856	0.02856
8	0.01934	0.01803	0.01739	0.01701	0.01688
16	0.01594	0.01167	0.01003	0.009247	0.008794
32	0.007324	0.005391	0.004471	0.003956	0.003794
64	0.005254	0.003095	0.002029	0.001441	0.001269

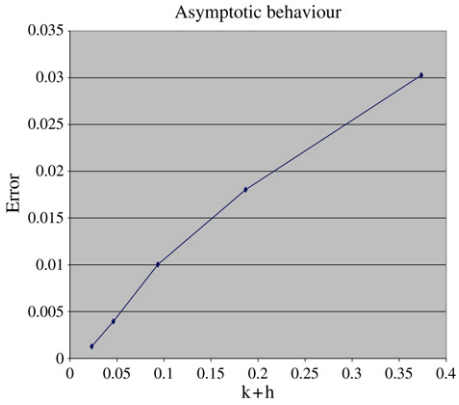

Fig. 3. Example I: Evolution of the numerical error with respect to $k + h$.

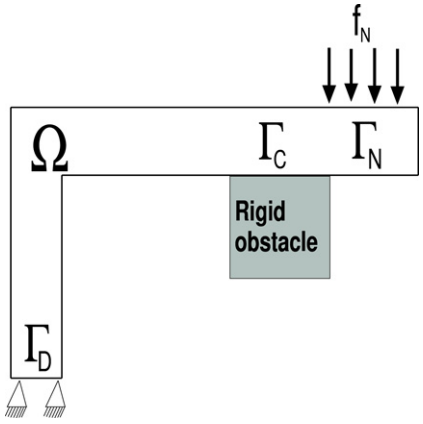

Fig. 4. Example II: Contact problem of an L-shaped domain.

The numerical errors given by

$$\max_{0\le n\le N}\left\{\|\boldsymbol{u}_n-\boldsymbol{u}_n^{hk}\|_V+\|\zeta_n-\zeta_n^{hk}\|_Y\right\}$$

are shown in Table 1 (here, $h=\frac{\sqrt{2}}{n}$ and $\boldsymbol{u}_n$ and ζ_n denote, as previously noticed, the discrete solutions obtained with parameters $h=\sqrt{2}/256$ and $k=10^{-4}$). As can be seen, the numerical convergence of the algorithm is obtained. Moreover, its linear convergence with respect to $h+k$, stated in Corollary 7, is almost observed in Fig. 3.

4.2. Example II: Damage in an L-shaped body

As the second example, we consider an L-shaped body which is subjected to the action of traction forces on its upper horizontal boundary. The body is clamped on its lower horizontal boundary and an obstacle is assumed to be in contact, i.e. $g=0$, on the boundary part Γ_C (see Fig. 4).

The following data have been used in the simulations:

$$T=1\,\mathrm{s},\quad \boldsymbol{f}_B=\boldsymbol{0}\,\mathrm{N/m^3},\quad \boldsymbol{f}_N(x_1,x_2,t)=(0,-80t)\,\mathrm{N/m^2},$$

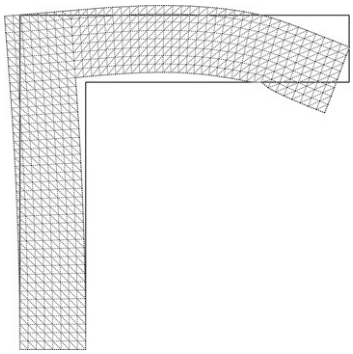

Fig. 5. Example II: Deformed mesh (amplified by 10) and initial configuration.

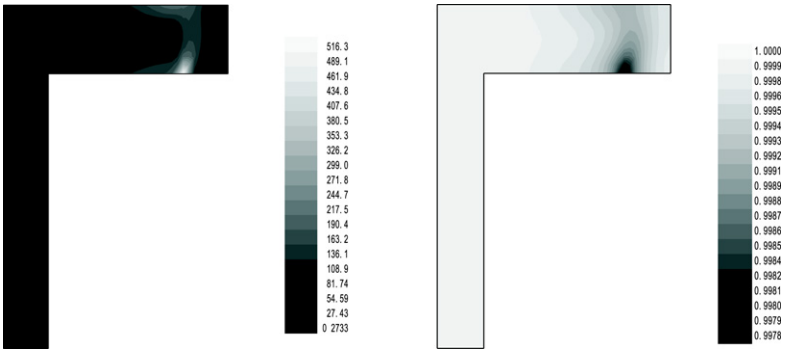

Fig. 6. Example II: Von Mises stress norm (left) and damage field (right) at final time.

$$\kappa = 1, \quad E = 10^5\ \mathrm{N/m^2}, \quad r = 0.3, \quad \zeta_* = 0.01,$$
$$\lambda_D = 5 \times 0.05, \quad \lambda_U = 10^3, \quad \lambda_W = 0, \quad \zeta_0 = 1.$$

The deformed mesh (amplified by 10) at final time and the initial configuration are plotted in Fig. 5. As we expected, the body bends because of the obstacle and we also observe that no penetration has been produced. Moreover, in Fig. 6 the von Mises stress norm (left-hand side) and the damage field (right-hand side) are depicted at final time. As can be seen, the most damaged areas coincide with the highest stressed ones, which are located near the contact areas.

4.3. Example III: Damage in a U-shaped domain

As the third example, our aim is the simulation of a simplified masonry bridge (see, for instance, [22]). Here, we use our model to obtain the most damaged areas which we identify with the possible breaking zones. Therefore, we consider the physical setting described in Fig. 7. A vertical force $\boldsymbol{f}_N(x_1, x_2, t) = (0, -80t)\ \mathrm{N/m^2}$ is acting on a part of the upper horizontal boundary, while the lower horizontal ones are assumed to be in contact with a rigid obstacle (again, $g = 0$ m).

The following data have been employed in the simulations:

$$T = 1\ \mathrm{s}, \quad \boldsymbol{f}_B = \mathbf{0}\ \mathrm{N/m^3}, \quad \boldsymbol{f}_N(x_1, x_2, t) = (0, -80t)\ \mathrm{N/m^2},$$
$$\kappa = 1, \quad E = 10^6\ \mathrm{N/m^2}, \quad r = 0.3, \quad \zeta_* = 0.01,$$
$$\lambda_D = 5 \times 0.05, \quad \lambda_U = 10^3, \quad \lambda_W = 0, \quad \zeta_0 = 1.$$

The deformed mesh (amplified by 10) at final time and the initial configuration are plotted in Fig. 8. As we expected, the body bends because of the applied forces. We also observe that no penetration has been produced and there was a sliding effect on the contact areas. Moreover, in Fig. 9 the von Mises stress norm (left-hand side) and the damage field (right-hand side) are depicted at final time. As can be seen, the most damaged areas coincide again with the highest stressed ones, which are located near the contact areas and where the body bends.

5. Conclusions

The paper dealt with the numerical analysis and simulations of a contact problem between an elastic body and a rigid obstacle. The evolution of the material damage, which led to the development and growth of micro-cracks, was also taken into account. A numerical algorithm for the model, based on finite elements and a hybrid combination of the backward

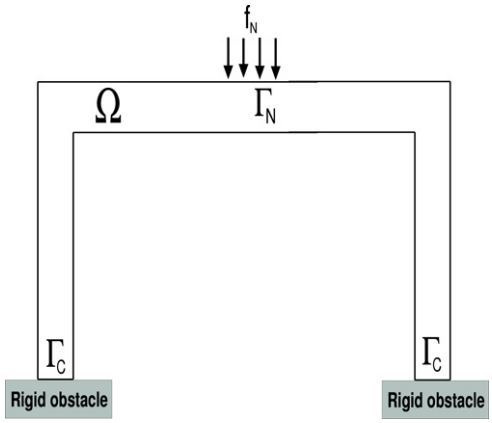

Fig. 7. Example III: Simulation of a U-shaped domain.

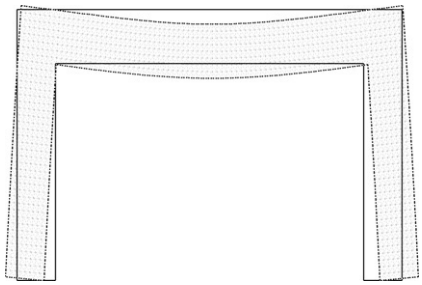

Fig. 8. Example III: Deformed mesh (amplified by 10) and initial configuration.

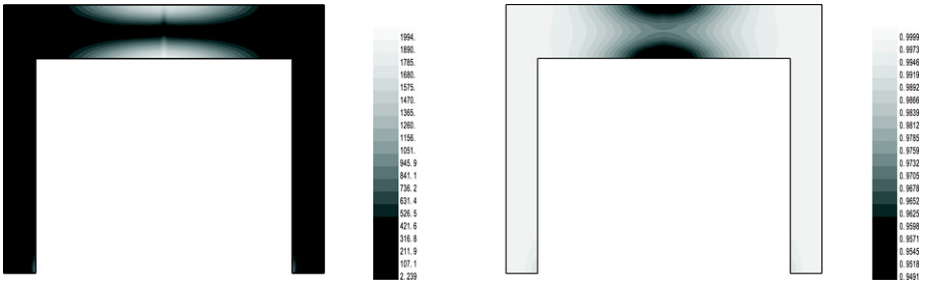

Fig. 9. Example III: Von Mises stress norm (left) and damage field (right) at final time.

and the forward Euler schemes, was proposed and error estimates on its solutions were obtained, from which the linear convergence, with respect to the discretization parameters, was derived.

We must notice that the error estimates provided in Corollary 7, which states the linear convergence of the algorithm for the case of continuous piecewise affine functions, were derived under an additional assumption on the regularity of the solution which was not proved. However, since for the case of contact with a deformable obstacle this regularity was improved (see [8]), we hope to address it in the near future.

The algorithm was implemented and three examples were computed. In the first one, the setting was chosen in such a way as to show the numerical convergence of the algorithm. As can be seen in Fig. 3, the linear convergence of the algorithm was achieved. In the second example, the aim was to study the location of the most damaged areas in an L-shaped body subjected to the action of surface forces. Finally, in the third example, a U-shaped body, representing a simplified masonry bridge, was simulated. In these last two examples, we observed that the most damaged areas coincided with the highest stressed ones.

Finally, we notice that the results presented in this paper could be easily extended to other contact problems including, for instance, friction, by using similar arguments to those employed in [10] in the case of viscoelastic materials. Moreover, although the computer implementation could be done in a similar way, the dynamical version of this problem (i.e, including the full dynamical mass term) will have additional mathematical issues such as the existence and uniqueness of weak solutions or developing useful error estimates that cannot be considered yet.

References

[1] T.A. Angelov, On a rolling problem with damage and wear, Mech. Res. Comm. 26 (1999) 281–286.
[2] K.T. Andrews, J.R. Fernández, M. Shillor, Numerical analysis of dynamic thermoviscoelastic contact with damage of a rod, IMA J. Appl. Math. 70 (6) (2005) 768–795.
[3] Z.P. Bazant, G. Pijaudier-Cabot, Nonlocal continuum damage, localization stability and convergence, J. Appl. Mech. 55 (1988) 287–293.
[4] A. Bermúdez, C. Moreno, Duality methods for solving variational inequalities, Comput. Math. Appl. 7 (1981) 43–58.
[5] E. Bonetti, M. Frémond, Damage theory: Microscopic effects of vanishing macroscopic motions, Comput. Appl. Math. 22 (3) (2003) 313–333.
[6] E. Bonetti, G. Schimperna, Local existence for Frémond's model of damage in elastic materials, Comp. Mech. Thermodyn. 16 (4) (2004) 319–335.
[7] M. Campo, J.R. Fernández, W. Han, M. Sofonea, A dynamic viscoelastic contact problem with normal compliance and damage, Finite Elem. Anal. Des. 42 (2005) 1–24.
[8] M. Campo, J.R. Fernández, K.L. Kuttler, An elastic-viscoplastic contact problem with damage, Comput. Methods Appl. Mech. Engrg. 196 (33–34) (2007) 3219–3229.
[9] M. Campo, J.R. Fernández, K.L. Kuttler, M. Shillor, Quasistatic evolution of damage in an elastic body: Numerical analysis and computational experiments, Appl. Numer. Math. 57 (9) (2007) 975–988.
[10] M. Campo, J.R. Fernández, J.M. Viaño, Numerical analysis and simulations of a quasistatic frictional contact problem with damage, J. Comput. Appl. Math. 192 (2006) 30–39.
[11] O. Chau, J.R. Fernández, W. Han, M. Sofonea, A frictionless contact problem for elastic-viscoplastic materials with normal compliance and damage, Comput. Methods Appl. Mech. Engrg. 191 (2002) 5007–5026.
[12] P.G. Ciarlet, The finite element method for elliptic problems, in: P.G. Ciarlet, J.L. Lions (Eds.), in: Handbook of Numerical Analysis, vol. II, North Holland, 1991, pp. 17–352.
[13] G. Duvaut, J.L. Lions, Inequalities in Mechanics and Physics, Springer-Verlag, Berlin, 1976.
[14] J.R. Fernández, Analysis of a one-dimensional damage model, Numer. Methods Partial Differential 21 (6) (2005) 1122–1139.
[15] M. Frémond, B. Nedjar, Damage in concrete: the unilateral phenomenon, Nuclear Eng. Des. 156 (1995) 323–335.
[16] M. Frémond, B. Nedjar, Damage, gradient of damage and principle of virtual work, Internat. J. Solids Structures 33 (8) (1996) 1083–1103.
[17] M. Frémond, Non-smooth Thermomechanics, Springer, Berlin, 2002.
[18] M. Frémond, K.L. Kuttler, M. Shillor, Existence and uniqueness of solutions for a one-dimensional damage model, J. Math. Anal. Appl. 229 (1999) 271–294.
[19] R. Glowinski, Numerical Methods for Nonlinear Variational Problems, Springer, New York, 1984.
[20] W. Han, M. Shillor, M. Sofonea, Variational and numerical analysis of a quasistatic viscoelastic problem with normal compliance, friction and damage, J. Comput. Appl. Math. 137 (2001) 377–398.
[21] W. Han, M. Sofonea, Quasistatic Contact Problems in Viscoelasticity and Viscoplasticity, American Mathematical Society-Intl. Press, 2002.
[22] J. Heyman, The masonry arch, in: Ellis Horwood Series In Engineering Science, 1982.
[23] N. Kikuchi, J.T. Oden, Contact problems in elasticity: A study of variational inequalities and finite element methods, in: SIAM Studies in Applied Mathematics, vol. 8. Philadelphia, PA, 1988.
[24] K.L. Kuttler, Quasistatic evolution of damage in an elastic-viscoplastic material, Electron. J. Differential 147 (2005) 25 pp..
[25] K.L. Kuttler, M. Shillor, Quasistatic evolution of damage in an elastic body, Nonlinear Anal. Real World Appl. 7 (4) (2006) 674–699.
[26] K.L. Kuttler, M. Shillor, J.R. Fernández, Existence and regularity for dynamic viscoelastic adhesive contact with damage, Appl. Math. Optim. 53 (2006) 31–66.
[27] J. Lemaitre, R. Desmorat, Engineering Damage Mechanics: Ductile, Creep, Fatigue and Brittle Failures, Springer-Verlag, 2005.
[28] R. Liebe, P. Steinmann, A. Benallal, Theoretical and numerical aspects of a thermodynamically consistent framework for geometrically linear gradient damage, Comput. Methods Appl. Mech. Engrg. 190 (2001) 6555–6576.
[29] C. Miehe, Discontinuous and continuous damage evolution in Ogden-type large-strain elastic materials, Eur. J. Mech. A 14 (3) (1995) 697–720.
[30] B. Nedjar, Elastoplastic-damage modelling including the gradient of damage. Formulation and computational aspects, Internat. J. Solids Structures 38 (2001) 5421–5451.
[31] R.H.J. Peerlings, R. de Borst, W.A.M. Brekelmans, J.H.P. de Vree, Gradient-enhaced damage for quasi-brittle materials, Internat. J. Numer. Methods Engrg. 39 (1996) 3391–3403.
[32] M. Shillor, M. Sofonea, J.J. Telega, Models and Analysis of Quasistatic Contact, in: Lecture Notes in Physics, vol. 655, Springer, Berlin, 2004.
[33] P. Steinmann, Formulation and computation of geometrically non-linear gradient damage, Internat. J. Numer. Methods Engrg. 4 (1999) 757–779.
[34] P. Steinmann, C. Miehe, E. Stein, Comparison of different finite deformation inelastic damage models within multiplicative elastoplasticity for ductile materials, Comput. Mech. 13 (1994) 458–474.